Cell, Vol. 103, 169–179, September 29, 2000, Copyright ©2000 by Cell Press

Accessory Protein Facilitated CFTR-CFTR Interaction, a Molecular Mechanism to Potentiate the Chloride Channel Activity

Shusheng Wang,* Hongwen Yue,* Rachel B. Derin,* William B. Guggino,* and Min Li†‡
*Department of Physiology
†Department of Neuroscience
The Johns Hopkins University School of Medicine
725 North Wolfe Street
Baltimore, Maryland 21205

Summary

The *c*ystic *f*ibrosis *t*ransmembrane conductance *r*egulator (*CFTR*) gene encodes a chloride channel protein that belongs to the superfamily of *A*TP *b*inding *c*assette (ABC) transporters. Phosphorylation by protein kinase A in the presence of ATP activates the CFTR-mediated chloride conductance of the apical membranes. We have identified a novel hydrophilic CFTR binding protein, CAP70, which is also concentrated on the apical surfaces. CAP70 consists of four PDZ domains, three of which are capable of binding to the CFTR C terminus. Linking at least two CFTR molecules via cytoplasmic C-terminal binding by either multivalent CAP70 or a bivalent monoclonal antibody potentiates the CFTR chloride channel activity. Thus, the CFTR channel can be switched to a more active conducting state via a modification of intermolecular CFTR-CFTR contact that is enhanced by an accessory protein.

Introduction

The *A*TP *b*inding *c*assette (ABC) superfamily proteins are important functional transporters in both prokaryotes and eukaryotes, playing the primary roles in mediating the entry and exit of a variety of molecules. They form the largest group of paralogous proteins both in *Escherichia coli* with 80 members and in *Bacillus subtilis* with 78 members, implicating their critical roles in cellular physiology. Although the precise number is currently unknown, existing information also suggests that this family of proteins is highly represented in the human genome. Furthermore, abnormal function of ABC transporters has been directly linked to the causes of several human diseases.

Cystic fibrosis (CF) is an autosomal recessive disorder caused by mutations in the *CFTR* gene, which encodes a chloride-conducting channel (Riordan et al., 1989; Drumm et al., 1990; Rich et al., 1990). The CFTR protein is a paradigmatic member of ABC transporters. Like other ABC transporters, CFTR comprises two hydrophobic core regions, where each contains six putative membrane-spanning segments and two nucleotide binding domains (NBDs). Unique to CFTR is an additional large cytoplasmic domain (R domain) connecting the first and second halves of the CFTR molecule (Riordan et al., 1989). The cloned *CFTR* gene encodes a chloride channel that is activated by phosphorylation of the R domain by cAMP-activated kinases (PKA), and agonistic ATP binding to and hydrolysis by the NBD domain(s) (Frizzell et al., 1986; Gadsby et al., 1995).

The genetic cause of human cystic fibrosis by *CFTR* mutations has been well established (see review by Zielenski and Tsui, 1995). Physiological experiments have suggested that the native CFTR channel is a macromolecular complex that can be regulated by various accessory-interacting proteins (see reviews by al-Awqati, 1995 and Wine, 1995). Like many other members of the ABC transporter superfamily, the precise stoichiometry of the CFTR channel is not known.

Using a combination of biochemical and molecular techniques, we have identified a multivalent CFTR binding protein, CAP70, which is capable of facilitating intermolecular CFTR interaction. By directly testing its effects on the CFTR channel activity, we found that dimeric binding to the C terminus of CFTR by the recombinant CAP70 protein or a monoclonal antibody is sufficient to potentiate the chloride current. Our results suggest that the CFTR channel is a dynamic macromolecular complex. The modulation of intermolecular contacts by a cytoplasmic accessory protein provides a molecular basis for their functional plasticity.

Results

Identification of CAP70

The C-terminal amino acid sequences of CFTR predicted from the cloned genes are highly conserved among many species (Figure 1a). To test the hypothesis that the C-terminal region may be involved in the interaction with accessory proteins, an affinity column using glutathione S-transferase (GST) fusion was constructed which contained the 15 C-terminal residues of the human CFTR protein (Figure 1a). The binding proteins specific for the CFTR affinity column were purified from mouse kidney extracts. When separated on SDS-PAGE, at least four polypeptides specific for the GST-CFTR column were identified. These *C*FTR-*A*ssociated *P*roteins (CAPs) had molecular masses of 40, 55, 70, and 85 kDa (Figure 1b). The binding specificity to the CFTR C terminus was demonstrated by the restricted association with GST-CFTR beads, but not GST alone beads. The individual CAPs could interact either directly with the CFTR C terminus or indirectly through association with another CAP.

On the basis of the intensity of the Coomassie stain, CAP70 was the most abundant polypeptide retained by the affinity column and it thus served as a good candidate for direct interaction with the CFTR C terminus. To determine the amino acid sequence, a large-scale purification was carried out. The resultant purified proteins were fractionated on SDS-PAGE, and transferred and immobilized onto a polyvinylidene difluoride (PVDF) membrane. To avoid potential N-terminal protection, the CAP70 polypeptide on the membrane was digested in

‡To whom correspondence should be addressed: (e-mail: minli@jhmi.edu).

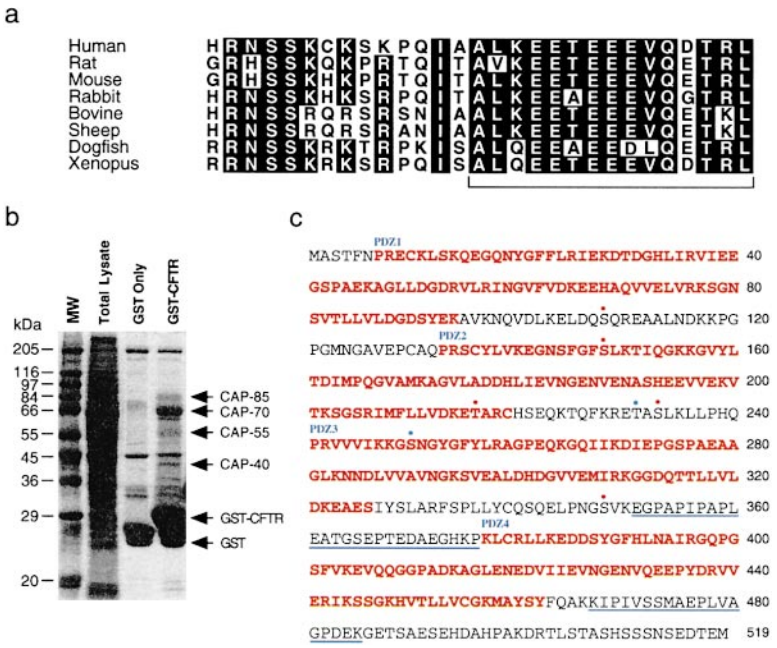

Figure 1. Identification of CAP70

(a) Amino acid sequence alignment of the C termini of *CFTR* from human (P13569), rat (382755), mouse (M60439), rabbit (Q00554), bovine (P35071), sheep (U20418), dogfish (P26362), and *Xenopus* (U60209). The last 15 residues are bracketed. Conserved residues are highlighted.

(b) Affinity purification of the *C*FTR-*A*ssociated *P*roteins (CAPs). The last 15 amino acids of CFTR were fused to GST to form GST-CFTR (1466-1480). Protein samples from different preparations (marked on the top) were separated by SDS-PAGE and visualized by Coomassie staining. Molecular weight standards and various CAPs are indicated on the left and right sides of the panel, respectively.

(c) Deduced amino acid sequence of mouse *CAP70*. The residues corresponding to the two tryptic peptides from the purified CAP70 protein are underlined. The four PDZ domains, PDZ1 to PDZ4, are highlighted in red. Potential sites for phosphorylation by protein kinase A and protein kinase C are marked with blue and red dots, respectively.

situ and the released tryptic peptides were purified by HPLC. Microsequencing of internal tryptic peptides from the purified CAP70 revealed two sequences of 26 residues and 19 residues, respectively (Figure 1c). Although the tryptic peptides did not identify any known genes in the database, comparison of the peptide sequences with those in NCBI databases revealed several expression sequence tag (EST) clones. The sequence analyses of the full-length cDNA revealed that *CAP70* was a mouse homolog of *PDZK1*. *PDZK1* is a human gene identified in a yeast two-hybrid screen using MAP17 as bait. MAP17 was initially identified by using the differential display technique that was selected for genes upregulated in renal cell carcinoma compared with normal renal parenchyma. The function of MAP17 is currently unknown (Kocher et al., 1998).

CAP70 contained an open reading frame of 519 amino acids with a predicted molecular mass of 56 kDa. The deduced mouse CAP70 (mCAP70) amino acid sequence contained the two tryptic peptides, which confirmed that the two peptides were indeed derived from one protein (Figure 1c). CAP70 protein comprises four PDZ domains, which are also known as GLGF repeats, or disks-large homology repeats (DHRs) (see reviews by Kennedy, 1995 and Sheng, 1996). PDZ domains belong to a family of protein binding modules that have been shown to interact with target proteins through binding either to the C termini (Kim et al., 1995) or less commonly to internal regions (van Huizen et al., 1998; Hillier et al., 1999). Recent reports have shown that PDZ domains have diverse peptide binding specificity (Songyang et al., 1997; Stricker et al., 1997). The tandem arrangement of four PDZ domains suggests that CAP70 is likely to function by binding to multiple proteins to organize a macromolecular complex.

Tissue distribution of the human CAP70 messenger RNA was examined using Northern blot analysis. The 2.7 kb CAP70 transcript was found mainly in kidney, liver, and small intestine (Figure 2a). To further investigate the expression pattern, an antibody against mCAP70 was developed and affinity purified. This antibody specifically recognized a 70 kDa polypeptide, and strong immunoblot signals were consistently found in kidney, liver, and small intestine. A significant amount of CAP70 protein could be detected in brain, lung, and testis (Figure 2b). In addition, a relatively low level of 70 kDa polypeptide could also be detected from pancreas, stomach, and colon after longer exposure (data not shown). The expression pattern of *CAP70* partially overlapped with the tissue distribution of CFTR (Riordan et al., 1989; Trezise and Buchwald, 1991).

The subcellular localization of CAP70 was mainly restricted to apical domains of epithelial cells as demonstrated by immunofluorescence staining (Figure 2c). In kidney and small intestine, a dense staining of CAP70 was colocalized along the brush border (apical membrane domains) as revealed by the rhodamine-conjugated phloidin staining (Figure 2c, panels A–F). In kidney, the distribution of CAP70 was restricted mainly to the proximal tubules. The surrounding glomerulus and other tubular structures did not contain a significant level of CAP70 (Figure 2c, panels A–C). In both tissue samples, the staining could be abolished by antigen, i.e., the purified CAP70 (data not shown). The tissue and subcellular distribution of CAP70 was consistent with the CFTR localization (Crawford et al., 1991; Trezise and Buchwald, 1991; Denning et al., 1992), thus in agreement with the potential association of CAP70 with CFTR in vivo.

Interaction between CAP70 and CFTR

To determine whether and which region of CAP70 is responsible for direct interaction with the C terminus of CFTR, individual PDZ domains were expressed as hemagglutinin (HA) and green fluorescent protein (GFP)-fusions in human embryonic kidney (HEK) 293 cells (Figures 3a and 3b). The protein lysates of transfected

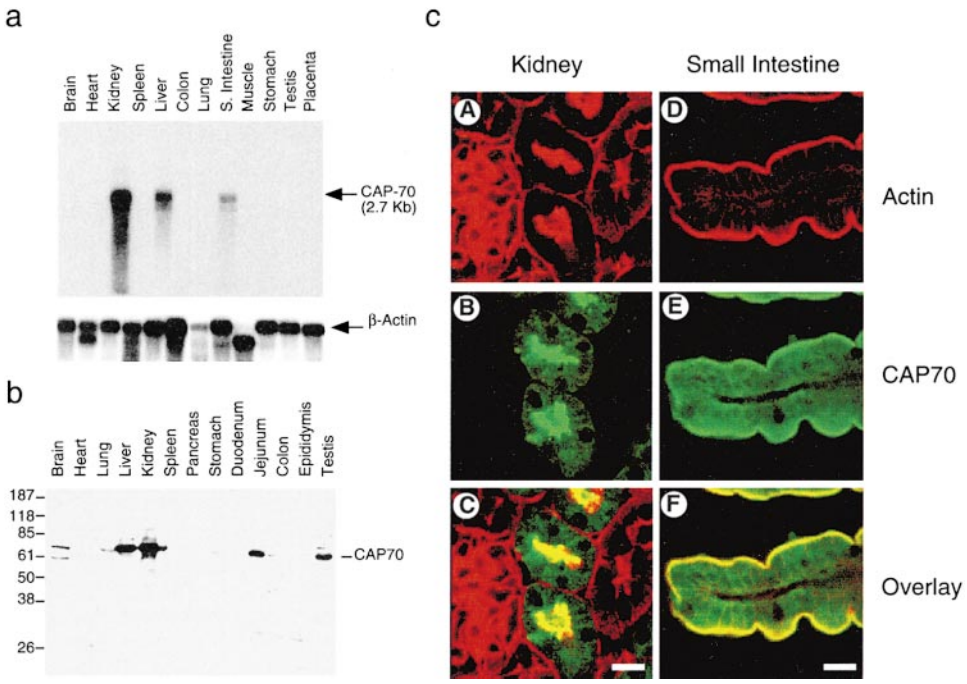

Figure 2. Tissue Distribution and Subcellular Localization of CAP70

(a) Tissue distribution of CAP70 mRNA assayed by Northern blot analysis. Poly(A)$^+$ RNA samples from indicated human tissues on the nitrocellulose membrane (Origene Technologies Inc., MD) were hybridized with hCAP70 (upper panel). After removing the bound probe, the filter was hybridized with a β-actin probe (bottom panel).

(b) Tissue distribution of the mCAP70 protein. Total protein lysates (20 μg protein) from the indicated tissues were separated by SDS-PAGE. The mCAP70 protein was detected by immunoblot analysis using purified rabbit anti-CAP70 antibody. The molecular weight standards are marked on the side.

(c) in vivo localization of mCAP70. Tissue sections from mouse kidney (A–C) and small intestine (D–F) were stained with anti-CAP70 antibody (B and E). Rhodamine-conjugated phloidin (0.1 μg/ml, Sigma) was used to highlight the brush borders of kidney (A) and small intestine (D). Overlays of anti-CAP70 and actin stainings are shown in panels (C) and (F). Bars = 10 μm.

HEK293 cells were tested for association with the CFTR C terminus by an affinity "pull-down" assay. Figure 3b shows that PDZ1, PDZ3, and PDZ4 could be precipitated by glutathione agarose beads with bound GST fusion of the CFTR C terminus (lanes 3), but not by GST beads alone (lanes 2). The binding affinity (K_D) was measured by surface plasmon resonance (SPR) method using a synthetic peptide (EEVQDTRL, C-peptide-TRL) corresponding to the last eight amino acids of CFTR and the purified GST fusion proteins of the individual PDZ domains (Figure 3a). The binding affinity varied from 8 nM of PDZ3 to 220 nM of PDZ1. Mutation of C-peptide-TRL to TRA abolished the interaction (data not shown). Thus, the CFTR-CAP70 interaction could be mediated through independent binding of the PDZ1, PDZ3, and PDZ4 domains of CAP70 to the C terminus of CFTR.

The multivalent binding capability may provide a mechanism for CAP70 to assemble multiple CFTR molecules. To test this hypothesis, we coexpressed CAP70 in HEK293 cells with the CFTR C-terminal domains that were differentially tagged with either HA epitope (HA-CFTR-Ct) or green fluorescent protein (GFP-CFTR-Ct) (Figure 3c). Multimerization of the CFTR C-terminal domain by CAP70 was assessed based on whether HA-CFTR-Ct can be coimmunoprecipitated with GFP-CFTR-Ct in the presence of CAP70. Figure 3d shows that HA-CFTR-Ct was precipitated by an anti-GFP antibody only upon the coexpression of CAP70 (Figure 3d, upper panel). Substitution of the terminal TRL with TRA (HA-CFTR-Ct*), which eliminated the CAP70-CFTR interaction (data not shown), abolished the coprecipitation under the same conditions (Figure 3d, lower panel). The data show that CAP70 is capable of nucleating a protein complex that contains more than one CFTR C-terminal domain. The recruitment of CFTR into the complex requires its ability to bind to CAP70. We also attempted the above experiment using differentially tagged full-length CFTR constructs. A combination of nonspecific CFTR aggregation and differential expression level of CAP70 and full-length CFTR fusions in transiently transfected cells rendered the experiment unsuccessful (data not shown).

To further investigate the interaction of CAP70 with CFTR in a cellular environment, HEK293 cells were transfected with functional GFP-CFTR in the presence or absence of CAP70. The transfected cells were lysed and immunoprecipitated with an affinity-purified anti-CAP70 antibody. The immunoprecipitates were then labeled with PKA in the presence of [^{33}P]-γ−ATP and resolved by SDS-PAGE. The GFP-CFTR fusion could be immunoprecipitated with the anti-CAP70 antibody only in cells that were cotransfected with CFTR and CAP70 (Figure 3e).

To investigate the potential native association of

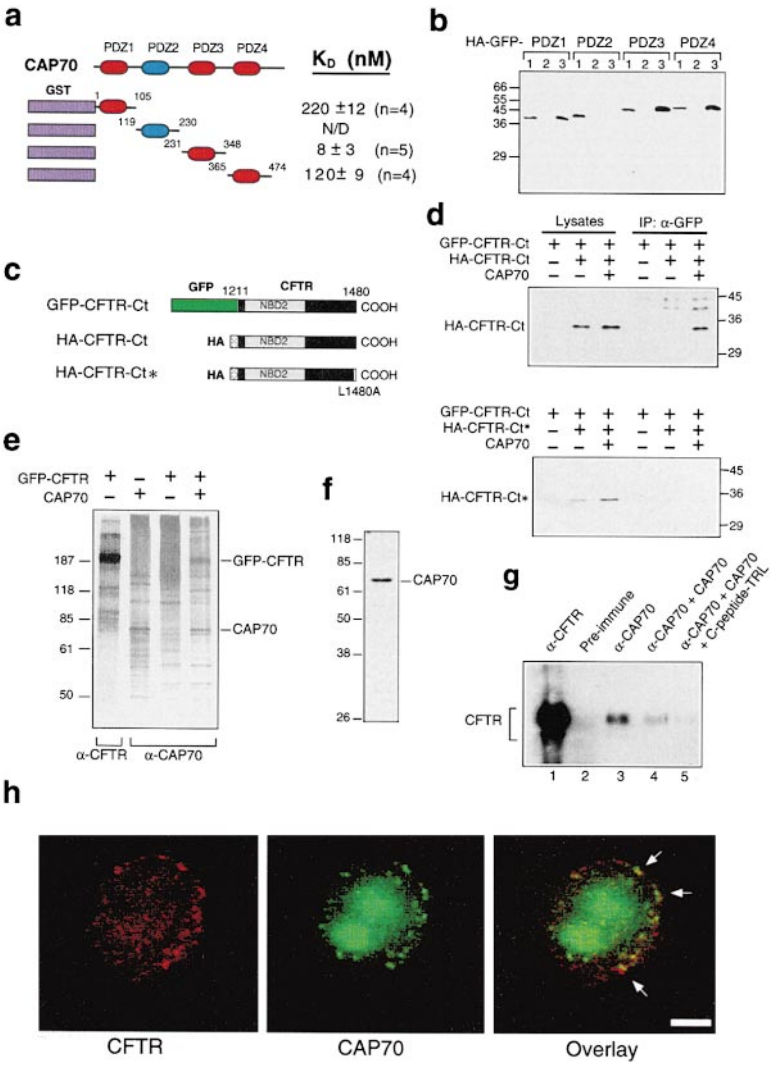

Figure 3. Interaction between CAP70 and CFTR

(a) Schematic diagrams of the constructs for four GST-PDZ fusions. The amino acid positions corresponding to CAP70 coding sequence are indicated. CAP70 possesses three distinct binding sites for CFTR and the binding affinity (K_D) is shown on the right.

(b) The affinity "pull-down" assay. The GST-CFTR (1466-1480) bound beads were incubated with cell lysates from four HA-GFP-tagged PDZ domains as indicated on the top. The expressed PDZ fusions (as shown in [a]) were detected with anti-HA monoclonal antibody. Lanes 1 are input lysates; lanes 2, proteins bound to GST-beads; lanes 3, proteins bound to GST-CFTR (1466-1480) beads.

(c) Schematic diagrams of GFP and HA-fusions of the wild-type and mutant CFTR C terminus. The amino acid positions corresponding to the CFTR coding sequences are indicated. The amino acid substitution of leucine with alanine at the C-terminal end (L1480A) was designated as HA-CFTR-Ct*.

(d) Multimerization of CFTR C termini by CAP70. The cells were cotransfected with various combinations of plasmids as indicated on the top. Immunoprecipitates were washed in the presence of 0.75 M NaCl, separated by SDS-PAGE, and probed with the anti-HA monoclonal antibody.

(e) Coimmunoprecipitation of CAP70 and CFTR from transfected HEK293 cells. The cells were transfected with various combinations of plasmids as shown on the top. The antibodies (~1 μg) used in immunoprecipitation are indicated at the bottom. The immunoprecipitates were radiolabeled by [γ-^{33}P]ATP and PKA and resolved by 7.5% SDS-PAGE.

(f) Detection of CAP70 in Calu-3 cell lysates by immunoblot analysis using an anti-human CAP70 antibody (1:1000 dilution).

(g) Coimmunoprecipitation of CAP70 and CFTR from the airway epithelial cell line, Calu-3. The amount of antibodies and proteins used in each reaction is as follows: 1 μg of anti-CFTR R/C terminus, 5 μl of preimmune serum, 1 μg of anti-human CAP70, 5 μg of purified CAP70 and 2.5 μg of CFTR C-peptide-TRL. The immunoprecipitates were resolved by 5% SDS-PAGE, transferred to PVDF membrane, and detected by immunoblot analysis using anti-CFTR C-terminal antibody (1:1000 dilution, Genzyme, MA).

(h) Colocalization of CFTR and CAP70 in primary cultured human bronchial airway epithelial cells. Cells were grown on collagen-coated cover slips and stained with an anti-CFTR R domain antibody (1:200 dilution, Genzyme, MA) and an anti-hCAP70 antibody (1:100 dilution). The specificity of anti-hCAP70 staining was tested by competition with excessive amount of antigen, i.e., CAP70. Colocalization of CAP70 (FITC-labeled) with CFTR (Cy3-labeled) in the peripheral region indicated by arrows. Bar = 5 μm.

CAP70 and CFTR, coimmunoprecipitation experiments were performed using human airway epithelial cell line Calu-3, where functional expression of native CFTR was detected (e.g., Shen et al., 1994) and CAP70 protein was also found (Figure 3f). The CFTR protein was detected in the protein complex precipitated by anti-CAP70 antibody (Figure 3g). In contrast, the CFTR protein was not detectable using the preimmune serum. Furthermore, the signal of CFTR coimmunoprecipitated by anti-CAP70 antibody could be competed by the purified recombinant CAP70. The efficiency of the antigenic CAP70 competition was further enhanced when the CFTR binding sites in CAP70 were preblocked with excess amounts of the C-peptide-TRL.

The localization of native CAP70 and CFTR was examined using confocal microscopy of immunofluorescence stained primary culture derived from human bronchial epithelial cells. CAP70 is a protein that is more abundant than CFTR. Consistent with this notion, the result revealed that CAP70 partially colocalized with CFTR in discrete small clusters in the peripheral region of the cell (Figure 3h). The weaker staining signal of CFTR presumably resulted from the anti-R domain antibody because anti-C terminus antibody, which recognizes the same epitope as CAP70, is not useful for this study. Interestingly, CAP70-specific staining was also found in the perinuclear region. In contrast, the CAP70 protein in native tissue was restricted to apical region (Figure 2c). These results suggest that the localization of CAP70 and possibly the association of CFTR with CAP70 are regulated in vivo.

Potentiation of CFTR Channel Activity by CAP70

The functional effect of the CAP70 binding was examined by patch-clamp recording of the CFTR chloride channel activity using transiently transfected HEK293

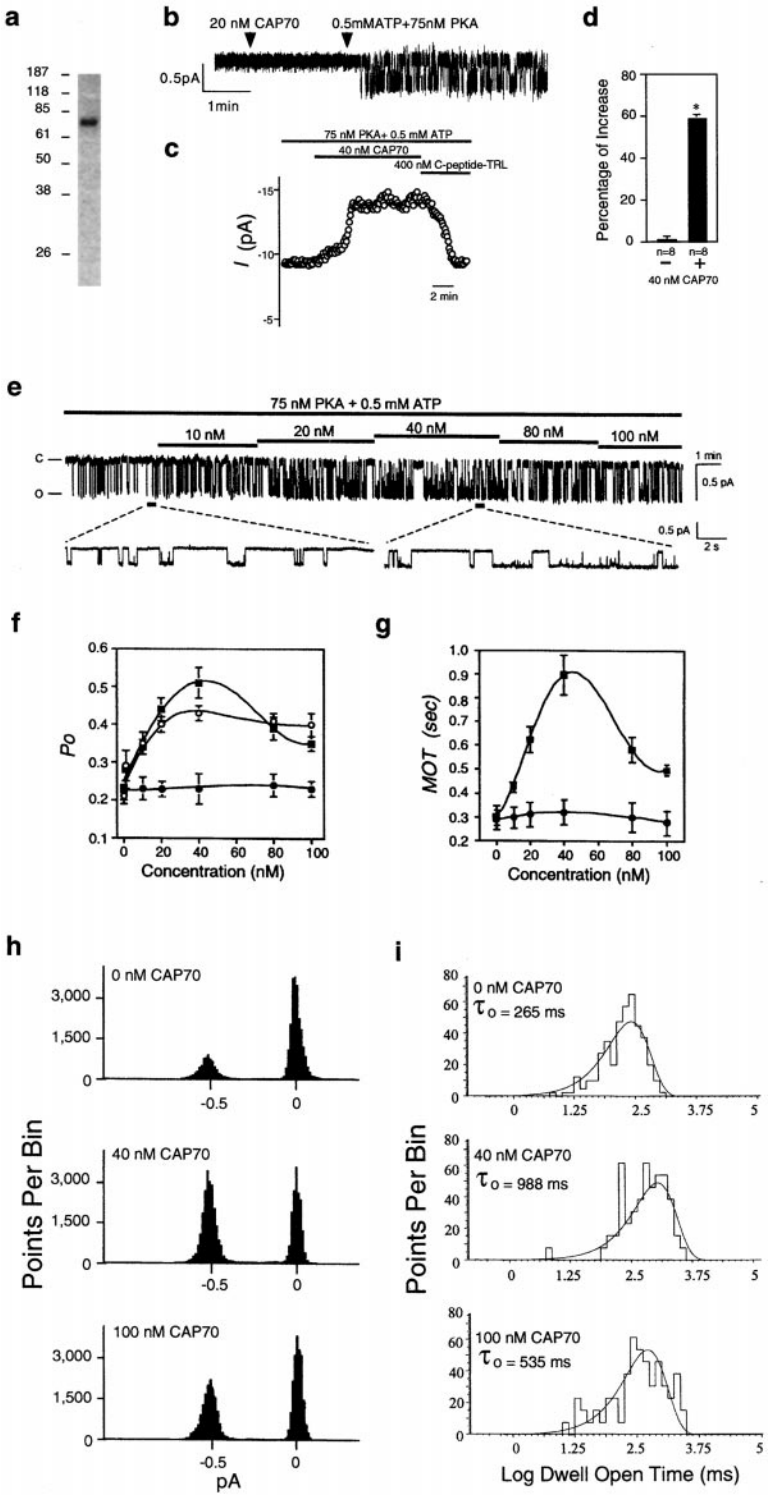

Figure 4. Effect of CAP70 on the Wild-Type CFTR Channel

(a) Expression and purification of recombinant CAP70. GST-fusion of full-length CAP70 was expressed in *E. coli* and cleaved by thrombin. The purified protein is shown after separation by 10% SDS-PAGE and detected by Coomassie staining. Molecular weight standards are shown on the left in kDa.

(b) Continuous single channel trace recorded in the presence of CAP70 alone and CAP70 with 75 nM PKA and 0.5 mM ATP. Arrows indicate the time point when CAP70 and PKA/ATP were added.

(c) Time course of Cl^- current in excised inside-out macropatches recorded in symmetrical bath solution (150 mM NMDG-Cl) after addition of 40 nM CAP70. Each data point represents mean current during a 6 s interval. 75 nM PKA and 0.5 mM ATP were present at all times as indicated by bars. The wash-out was performed in the continuous presence of PKA, ATP, and 400 nM of the CFTR C-peptide-TRL.

(d) Effect of CAP70 on CFTR activity. Values are mean current measured between 5 and 10 min after addition of CAP70. The asterisk indicates statistical significance ($p < 0.05$).

(e) A continuous current trace of wild-type CFTR channel from an excised inside-out patch in the presence of 75 nM PKA and 0.5 mM ATP. CAP70 was added into bath solution in a step-wise fashion as indicated. The selected traces representing in the absence and presence of CAP70 are expanded.

(f and g) Open probability (P_o) and mean opening time (MOT) of the wild-type CFTR and mutated CFTR-L1480A are plotted against different concentrations of purified recombinant CAP70 protein: filled squares, wild-type CFTR plus CAP70; filled circles, CFTR (L1480A) plus CAP70; open circles, wild-type CFTR plus PDZ3-3. Effect of the concatenated PDZ3-3 protein on P_o shown in (f). n for wild-type CFTR is 5~9, for CFTR/L1480A is 4 and for PDZ3-3 is 5.

(h) All point histograms are shown. The points/bin (vertical axis) are plotted against current (horizontal axis). The concentrations of CAP70 in each panel are as indicated.

(i) Dwell-time histograms are shown. The points/bin (vertical axis) are plotted against log dwell open time (horizontal axis). The open time histograms were fit by a single exponential function. The concentrations of CAP70 and time constants are as indicated in each panel.

cells. The CFTR current is PKA- and ATP-dependent and present only in transfected cells. The authenticity of the CFTR currents was further confirmed by the pharmacological behavior. The currents were insensitive to 4,4′-diisothiocyanostilbene-2,2′-disulfonic acid (DIDS) but could be inhibited by glybenclamide. The CAP70 used in this study was expressed in *E. coli* as a GST fusion and was purified to homogeneity after removing the GST portion by thrombin cleavage (Figure 4a). To test whether the recombinant CAP70 has any effect on the CFTR-mediated ion conducting activity, we studied the channel behavior using both single channel recording and macropatch recording techniques. Figure 4b shows a trace with typical CFTR characteristics, including linear current voltage relation, a 9.3 ± 0.1 pS (n = 19) conductance and the PKA- and ATP-dependent

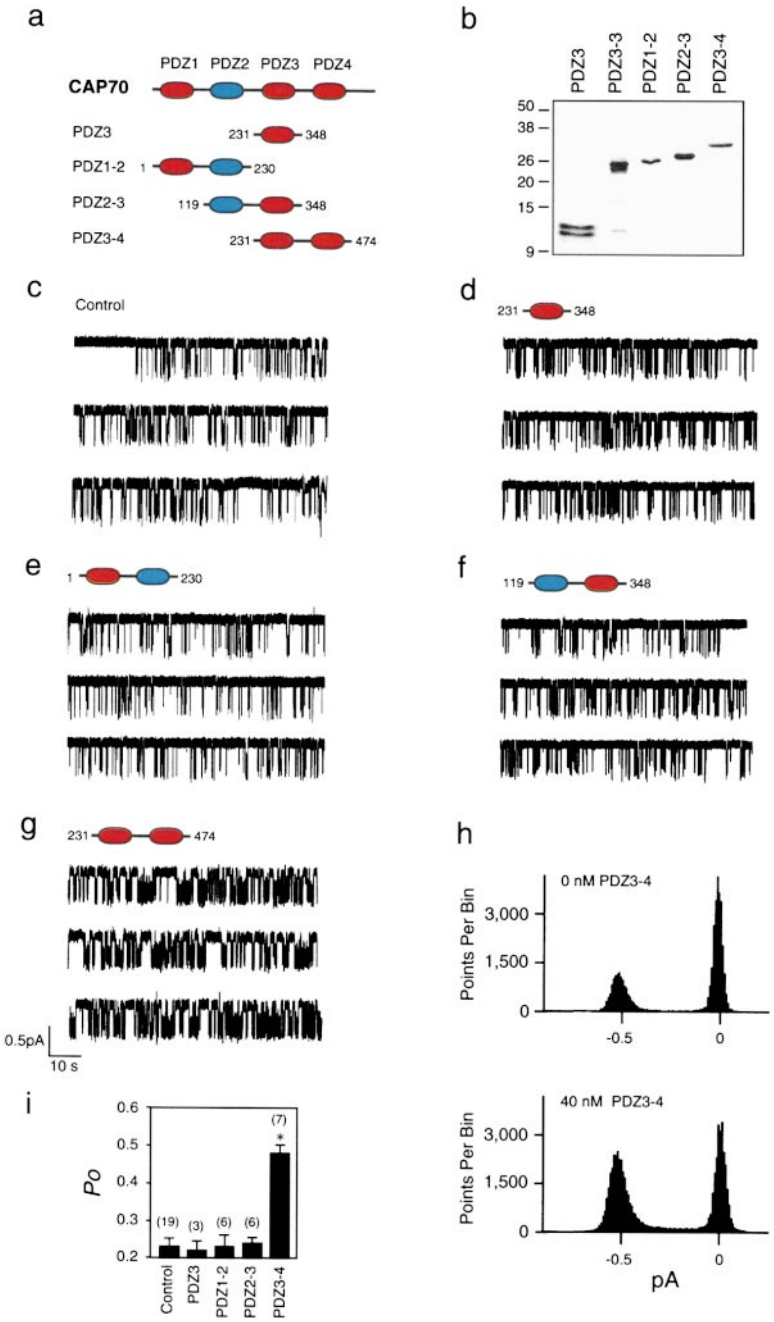

Figure 5. Mapping the Minimal Region of CAP70 Essential for Potentiation of CFTR

(a) Schematic diagrams of CAP70, PDZ3 (aa 231-348), PDZ1-2 (aa 1-230), PDZ2-3 (aa 119-348), and PDZ3-4 (aa 231-474). PDZ domains with CFTR binding ability are shown in red.

(b) Expression and purification of truncated CAP70 proteins. GST fusion of various truncated CAP70s were expressed in *E. coli* and cleaved by thrombin. The purified proteins were shown after separation by 12% SDS-PAGE and detected by Coomassie staining.

(c-g) Representative traces of single CFTR channel recordings in the absence (c) and presence of 40 nM of various truncated CAP70s: PDZ3 (d), PDZ1-2 (e), PDZ2-3 (f), and PDZ3-4 (g). CFTR channels were activated by PKA and ATP prior to the addition of the truncated CAP70s.

(h) All point histograms are shown. The points/bin (vertical axis) are plotted against the current (horizontal axis). The concentrations of purified PDZ3-4 in each panel are as indicated.

(i) Comparison of open probability (P_o) in the presence of various truncated CAP70s. Data shown are mean ± SE of P_o calculated from 3 min traces after the truncated CAP70s were applied to the patches. The initial 30 s after the addition of truncated CAP70s were excluded for the P_o analyses. The asterisk indicates statistical significance ($p < 0.05$). Numbers (n) of patches assayed are shown in parentheses.

channel opening. In the absence of PKA and ATP, CAP70 alone was not sufficient to activate the channel and had no effect on membrane conductance (Figure 4b). Under the inside-out macropatch configuration, application of CAP70 (40 nM) potentiated the CFTR chloride channel activity by nearly 60% (Figures 4c and 4d). The maximal potentiation was usually achieved in less than 5 min (Figure 4c). The potentiation was reversed within 2–3 min when the patched membrane was perfused with the competitive CFTR C-peptide.

To further characterize CAP70-mediated modulation, we studied the CAP70's effects using single channel recording techniques. The open probability (P_o) of CFTR channel was typically 0.23 ± 0.02 (n = 19) in the presence of 0.5 mM ATP. Upon application of the recombinant CAP70, the CFTR channel was switched to a more active state, where both open probability (P_o) and mean open time (MOT) increased in a dose-dependent manner (Figures 4f and 4g, closed squares). The potentiation reached a maximum at 40 nM of CAP70. A higher concentration of CAP70 induced a decline from the maximal potentiation, suggesting that the stoichiometry of the CAP70-CFTR complex plays a role in the optimal potentiation (see Figure 7 and Discussion). The CAP70-mediated potentiation was dependent on PKA and ATP. In the presence of 200 nM of peptide, only C-peptide-TRL (EEVQDTRL), and not mutated C-peptide-TRA (EEVQDTRA), was able to abolish the CAP70-mediated potentiation, consistent with the results of the binding experiments (data not shown). In addition, amino acid

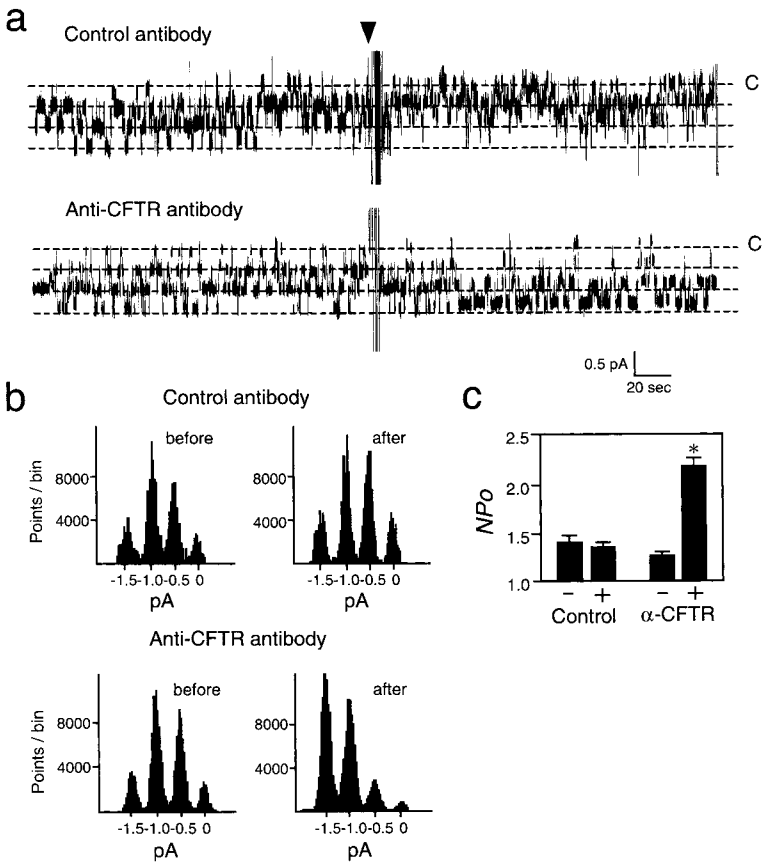

Figure 6. Effect of the Monoclonal Antibody on the CFTR Channel Activity

(a) The continuous traces represent 6 min recordings in the absence and presence of 40 nM of a control anti-HA monoclonal antibody (upper trace) and the monoclonal antibody specific to the C terminus of CFTR (Genzyme, MA) (bottom trace). The channel was activated in the presence of 75 nM PKA and 0.5 mM ATP. Addition of antibodies to the bath solution is indicated by an arrow.

(b) All point histograms are shown. The points/bin (vertical axis) are plotted against the current (horizontal axis). The antibodies used in the study are as indicated.

(c) Comparison of NP_o in the absence and presence of antibodies. Data shown are mean ± SE (n = 3) of NP_o calculated from the 3 min traces before and after the addition of 40 nM antibodies. The initial 30 ss after the addition of antibodies were excluded for NP_o analysis. The asterisk indicates statistical significance ($p < 0.05$).

substitution of the last residue leucine with alanine (L1480A) in CFTR, which abolishes the binding to CAP70, completely eliminated the CAP70-mediated potentiation (Figures 4f and 4g, closed circles), suggesting that the potentiation requires a direct interaction between CAP70 and the CFTR C terminus.

Purified CAP70 even at 250 nM behaved as a monomer as tested by gel filtration chromatography (data not shown). Results from the binding studies (Figure 3) showed that there were three CFTR interacting PDZ domains present in CAP70. To test for which one and how many interacting PDZ domains are necessary for the potentiation, the truncated CAP70 proteins corresponding to PDZ1–2, PDZ2–3, PDZ3–4, and PDZ3 (Figure 5a) were expressed and purified to apparent homogeneity (Figure 5b). These truncated proteins all displayed the ability to bind the C terminus of CFTR (Figures 3a and 3b). PDZ3, PDZ1–2, and PDZ2–3 each contain one CFTR binding site. When tested by excised inside-out patch recording, these truncated proteins were unable to induce any potentiation effect on the CFTR channel (Figures 5c-5f, i). In contrast, PDZ3–4, which contains two binding sites, displayed potentiation activity similar to that induced by the full-length CAP70 (Figures 5g-5i). These data showed that PDZ3–4 was sufficient to exert the potentiation activity.

The potentiation activity of the PDZ3–4 fusion could result from either bivalent binding of PDZ3–4 to two CFTR molecules, possible potentiation sequence motifs within the PDZ4 domain, or a combination of binding and potentiation sequence motifs. To distinguish between these possibilities, we tested the effect of a tandem PDZ3 domain protein (PDZ3–3) on CFTR channel activity. Figure 4f shows this tandem chimeric PDZ protein indeed exhibited the potentiation activity, which is consistent with the notion that bivalent binding is responsible for the potentiation.

To directly test whether the bivalent binding is sufficient for the potentiation, we used a monoclonal antibody that recognized the last four residues (DTRL-COOH) of CFTR. The bivalent binding by the antibody would bring two CFTR molecules in proximity, reminiscent of the bivalent binding ability of PDZ3–4 or PDZ3–3. Figure 6a shows that this antibody, a completely unrelated protein to CAP70, could also potentiate the channel activity (the lower trace). The antibody effects were abolished by competition of 100 nM of the C-peptide-TRL (data not shown). A control monoclonal antibody (anti-HA tag) at the same concentration did not show any such effect (the upper trace). This result demonstrated that the bivalent binding activity is sufficient for the potentiation, suggesting that CAP70 functions by modulating intermolecular CFTR-CFTR interaction. Such a configuration of dimeric CFTR gives rise to more active channels when activated by PKA and ATP.

Discussion

Structural studies of several prokaryotic ABC-like transporters have provided important biochemical insights into the function of this large family of proteins and their potential relevance to mutations in ABC transporters

that cause a variety of diseases (Armstrong et al., 1998; Hung et al., 1998). Because these structures are either partial or from nonparadigmatic transporters, the quaternary structure of mammalian ABC transporters remains largely unknown. Recent progress in low resolution structural studies has revealed images of purified multidrug resistant P-glycoprotein, suggesting that the monomeric form is sufficient for substrate binding and ATP hydrolysis (Rosenberg et al., 1997).

The CFTR protein regulates and is regulated by a variety of transporting processes. It has been speculated that the CFTR quaternary structure may also undergo dynamic changes. Thus, it is essential to determine the existence and organization of potential heteromeric and homomeric CFTR interactions with other functionally coupled proteins. Results consistent with possible homomeric CFTR-CFTR interaction include the finding that a tandem fusion of two CFTR coding sequences resulted in a functional channel which exhibited one single unitary conductance identical to that of CFTR (Zerhusen et al., 1999). In addition, electron microscopy studies revealed that the CFTR channel on the cell surface has a size that is considerably larger than that of a monomer (Eskandari et al., 1998). The result has also led to the suggestion that imaged particles are CFTR dimers. In contrast, biochemical studies on purified or coimmunoprecipitated protein showed that the purified recombinant CFTR protein is consistent with the monomeric channel or an unstable oligomer that could not survive the experimental procedures (Marshall et al., 1994). Furthermore, the purified P-glycoprotein was also seen as a monomer (Rosenberg et al., 1997). A possible explanation for the existing data is that the CFTR channel may interact to form a transitional dimer. Such a dimeric form is unstable, distinct from a typical multimeric channel complex such as a voltage-gated potassium channel, where the purified recombinant protein complex is stable and remains in a stoichiometry identical to its native form (Li et al., 1994).

The potentiation by recombinant CAP70 was dependent on the bivalent binding ability and not on a specific potentiation region of CAP70. Thus, modulation of the intermolecular CFTR interaction is an attractive mechanism for the potentiation activity. Figure 7 shows a proposed model for the CAP70-mediated potentiation. This model predicts that CFTR, in the absence of CAP70, exists either as a monomer or as a transient dimer when activated by PKA and ATP. In the presence of CAP70, the formation of CAP70-$(CFTR)_1$ allows for a more effective association with an additional CFTR molecule because the bound CAP70 provides at least two possible beneficial effects: (1) added affinity via either a PDZ1 or a PDZ4 association with another CFTR molecule, and (2) improved contact geometry between the two interacting CFTR molecules. The CAP70-configured $(CFTR)_2$ complex, when activated by PKA phosphorylation and agonistic ATP, induces a more active CFTR channel. Thus, the model also predicts that with an increasing CAP70 concentration, the highest affinity PDZ3 domain begins to dominate the binding. Under such conditions, although CAP70 remains in complex with CFTR, the bivalent CAP70-$(CFTR)_2$ configuration is less favorable. As a result, the potentiation by CAP70 will become less pronounced. Consistent with this model, a high concentration of CAP70 showed significantly reduced potentiation (Figures 4f–4i). The third prediction from this model is that a bivalent binding of two PDZ domains with equally high affinity would stabilize the CFTR-CFTR interaction. Therefore, we should not observe the aforementioned decline. Instead, the potentiation would reach a plateau phase with a less pronounced decline phase even at higher concentrations. Consistent with this prediction, the effect of the tandem PDZ protein of PDZ3-PDZ3 induced potentiation followed by a plateau phase at higher concentrations (Figure 4f, open circles). The binding affinity of PDZ3 is significantly higher than that of PDZ1 or PDZ4 (Figure 3a). However, the concentration of PDZ3-PDZ3 required for the maximal potentiation was not significantly lower than that of CAP70 despite the expected higher affinity (avidity) to CFTR. This inconsistency may be due to potential unfavorable constraints as a result of the chimeric construction. While the mechanistic details by which CAP70 potentiates the CFTR channel require further investigation, it would be particularly interesting to test the potential role of the parallel contact geometry of two NBD2 domains as a result of CAP70 binding.

A single conductance pore was observed by expres-

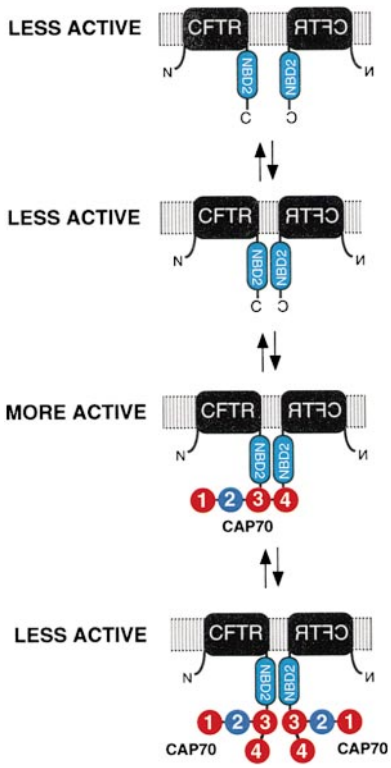

Figure 7. A Proposed Model of CAP70-Mediated Potentiation on the CFTR Channel

CFTR monomers have an intrinsic ability to interact with each other. CAP70 facilitates the CFTR-CFTR interaction via bivalent binding to the C termini of CFTR. The dimerization of CFTR enhanced by CAP70 or monoclonal antibody allows for a more active channel upon PKA and ATP stimulation. At high concentrations, CAP70 binding is mediated primarily via the PDZ3 domain, which has the highest affinity. As a result, the bivalent binding is reduced and the channel switches back to a less active state.

sion of tandem dimeric CFTR constructs (Zerhusen et al., 1999). While the data are consistent with the notion of CFTR-CFTR intermolecular contacts, the engineered covalent dimerization resulted in a less active channel. Such a reduction is possibly due to unfavorable geometry as a result of the head–tail linkage of the two CFTR molecules, whereas both CAP70 and the antibody mediate a tail–tail configuration of the CFTR-CFTR interaction.

In addition to CAP70, *N*a$^+$-*H*$^+$ *e*xchanger *r*egulatory *f*actor (NHE-RF), also known as EBP50 (*e*zrin *b*inding *p*rotein of 50 kDa), is the first protein to be reported to bind to the C terminus of CFTR (Hall et al., 1998; Short et al., 1998; Wang et al., 1998). This protein contains two PDZ domains (PDZ1 and PDZ2) with distinct peptide binding specificity as determined by random peptide display techniques; and the binding consensus of PDZ1 matches the sequence of the C terminus of CFTR (Wang et al., 1998). Although the functional role and native association of NHE-RF with CFTR have not been fully established, the heterogeneity in tissue distribution and domain organization of CAP70 and NHE-RF may allow them to act differentially in different cells or combinatorially within the same cell. This would provide an advantageous mechanism to confer the diverse regulation of the CFTR protein in terms of both its subcellular targeting and macromolecular organization.

Cytoplasmic binding of channel subunits by accessory proteins has been seen in several systems including *p*ostsynaptic *d*ensity 95 (PSD-95) mediated specific subcellular organization of potassium channel and NMDA receptors (Kim et al., 1995; Kornau et al., 1995). Our data suggest that, in addition to their cellular functions such as specifying subcellular localization and regulating channel density, accessory proteins may also provide a structural framework to establish conducting geometry and stoichiometry of ion channel and transporter complexes that control and regulate their functional heterogeneity.

Experimental Procedures

Purification of CAPs and Molecular Cloning of CAP70s

Mouse kidney extracts were prepared by homogenization in HNT buffer containing 20 mM HEPES-KOH (pH 7.5), 120 mM NaCl, 1% Triton X-100, 5 mM EDTA, 0.5 mM dithiothreitol (DTT), and a cocktail of protease inhibitors. The supernatant was collected after centrifugation of the lysate at 27,000 × g for 15 min at 4°C and incubated with a GST or GST-CFTR fusion protein bound to glutathione-agarose beads. After gentle rotation for 1 hr at 4°C, the beads were washed at 4°C, once with HNT buffer, twice with HNT buffer supplemented with 0.5 mM NaCl, and three times with HNT buffer without Triton X-100. Prior to SDS-polyacrylamide gel electrophoresis (PAGE), the bound material was eluted with an SDS sample buffer. After electrophoretic transfer to the PVDF membrane, the membrane-bound proteins were identified. The area corresponding to the CAP70 polypeptide was collected and subjected to tryptic digestion. After purification by HPLC, peptide sequences were determined by microsequencing (Wistar Institute, PA). The partial cDNA fragments were identified from EST database with the peptide sequences. The full-length mCAP70 cDNA was cloned from a kidney cDNA library.

Northern and Western Blots

Northern blots containing 2 μg of human mRNA from multiple tissues (Origene Technologies Inc., MD) were hybridized under high stringency with a ^{32}P-labeled probe made with the coding sequence of the human CAP70. The Western blot analysis was performed as described by Wang (Wang et al., 1998).

Plasmid Construction

Expression of GST, HA-tagged, or HA-GFP-tagged fusion was carried out by high-fidelity PCR (Elongase™, Life Technology) with primers containing in-frame restriction enzyme sites. The PCR products were digested and cloned into either a pGEX4T3 vector (Amersham-Pharmacia), a pCGN vector (Wang et al., 1998), or a pGFP vector (ClonTech Inc., CA). All PCR primer sequences are available upon request. Two PCR fragments, containing CAP70 coding sequences of aa 231–361 and aa 231–348, were fused at the XbaI site in the pGEX4T3 vector to produce a GST-PDZ3–3 fusion protein. The full-length CFTR was constructed into a pRSV vector as previously described (Devidas et al., 1998). The CFTR-L1480A was derived from the pRSV-CFTR by replacing the HpaI/ApaI fragment with a corresponding PCR fragment in which leucine 1480 was substituted with alanine. The resultant constructs were confirmed by DNA sequencing.

Antibody Preparation

To generate anti-sera against human and mouse CAP70 proteins, the full-length cDNAs were subcloned into the pGEX4T3 vector. The GST-CAP70 fusion protein was used to immunize rabbits (Strategic Solutions, CA). The antisera were purified on affi-gel 15 columns (Bio-Rad, CA) coupled with the purified CAP70 without GST. The antibodies were sequentially eluted in 0.1 M glycine (pH 2.5) and 0.1 M triethylamine (pH 11.3). The eluates were neutralized with 1 M Tris-HCl (pH 8.0). The specificity of the anti-CAP70 antibody was determined by immunoblot analysis. Monoclonal antibodies specific for the C terminus and R domain of CFTR were purchased from the Genzyme Corporation (MA). Anti-GFP antibody was purchased from Clontech (Palo Alto, CA).

In Vitro Binding

To determine the affinity between CAP70 and CFTR, individual PDZ domains were expressed in *E. coli* and affinity purified using glutathione-agarose beads. The affinity of the CAP70-CFTR association was measured by the surface plasmon resonance (SPR) method using purified GST fusion proteins (as indicated) and a synthetic peptide corresponding to the last eight residues of CFTR. The affinity pull-down experiments were carried out according to procedures that are essentially identical to those used in the CAP70 purification.

Coimmunoprecipitation

Calu-3 and transfected HEK293 cells were used for coimmunoprecipitation. Cells were washed twice with PBS and lysed in HNT lysis buffer as described above. The supernatant was collected after centrifugation of the lysate at 27,000 × g for 1 min at 4°C and then first incubated with the affinity-purified antibodies at 4°C for 1 hr, and subsequently, incubated with 40 μl of a 1:1 slurry of protein G or protein A-Sepharose for 16 hr at 4°C. The protein A or G-antibody complex was spun down at 4000 × g for 1 min. The beads were washed once with HNT buffer, twice with HNT buffer supplemented with 0.5 M NaCl, and three times with HNT buffer without Triton X-100. To radioactively label the CFTR protein, the immunoprecipitates were incubated for 1 hr at 30°C in 20 μl of reaction mix containing 50 mM Tris-HCl (pH 7.5), 10 mM $MgCl_2$, 0.1 mg/ml BSA, 10 μCi of [^{33}P]- γ−ATP and 10 units of PKA (Sigma, MO). The beads were washed twice with HNT buffer. The bound material was eluted with the SDS sample buffer, then separated by SDS-PAGE. The precipitated CFTR signal was detected by either autoradiography or immunoblot.

Immunohistochemistry and Confocal Microscopy

Immunofluorescence was performed on 10 μm cryo-sections of mouse kidney and small intestines. Sections were fixed and stained with affinity-purified antibodies according to the standard methods (Ausubel et al., 1993). Confocal microscopy was performed on a Noran "OZ" confocal system and an Olympus inverted microscope using an Olympus 60× or 100× oil immersion objective lens. Double-stained specimens were excited at 488 nm (FITC) and 568 nm (Rhodamine) using a Kr/Ar laser with FITC-narrow and rhodamine-narrow

filter sets. Images were collected and processed, and merged in Noran Intervision software.

Patch-Clamp Recording

Single-channel patch-clamp recording was carried out in the excised inside-out patch-clamp configuration by using conventional procedures. Human *CFTR* was expressed transiently in human embryonic kidney (HEK293) cells using the LipofectAMINE™ reagent (Gibco BRL, NY). Cells were routinely recorded at 36–72 hr after transfection. Patch-clamp pipette electrodes were prepared using a two-stage vertical puller. When filled with the pipette solution, their resistance was 2–5 mΩ for macropatches or 10–20 mΩ for single channel patches. The seal resistance was 5–25 GΩ for macropatches and 10–100 GΩ for single channel patches. The bath solution contained 150 mM N-methyl-D-glutamine chloride, 1.1 mM $MgCl_2$, 2 mM EGTA, and 10 mM TES (pH 7.35 with Tris); the pipette solution contained 150 mM N-methyl-D-glutamine chloride, 0.5 mM $MgCl_2$, and 10 mM TES (pH 7.35 with Tris). To activate the CFTR channels, catalytic subunits of protein kinase A (75 nM, Promega, WI) and Mg^{2+}-ATP (0.5 mM, Sigma) were added to the bath solution of the excised inside-out patches. All single channel patch-clamp studies were performed at 25°C. The voltage was held at −50 mV. Currents were amplified with an Axopatch 200B patch-clamp amplifier and recorded on videotape for later analysis. Data were low-pass filtered at 100 Hz, digitized at 1 kHz, and analyzed by pCLAMP6.03 software. For analysis of open probability and open-close kinetics, patches containing less than four channels were used. The number of channels in each patch was determined from the maximum number of simultaneous channel openings observed during the course of an experiment that typically lasted 15–45 min. P_o was calculated from a current recording of at least 3 min duration. Lists of open and closed times were created using a conventional half-amplitude crossing criterion for event detection. Transitions of less than 1 ms duration were excluded from the analysis. Results are expressed as mean ± SE of n observations. Statistical significance was assessed using a paired or unpaired Student's t test as appropriate. Differences were considered statistically significant when $p < 0.05$.

Acknowledgments

We thank Drs. Craig Montell, Peter Gillespie, King-Wai Yau, and members of the Li laboratory for helpful discussions and comments on the manuscript; Drs. Bruce Stanton and Morgan Sheng for communicating unpublished results; and Robyne Butzner for assistance with manuscript preparation. This work is supported by grants (to M. L.) from the National Institutes of Health, Cystic Fibrosis Foundation, and an American Heart Association Established Investigator award. W. G. B. is supported by grants from the National Institutes of Health and from the Cystic Fibrosis Foundation. S. W. is supported in part by a postdoctoral fellowship from the Cystic Fibrosis Foundation.

Received April 26, 2000; revised August 2, 2000.

References

al-Awqati, Q. (1995). Regulation of ion channels by ABC transporters that secrete ATP. Science *269*, 805–806.

Armstrong, S.R., Tabernero, L., Zhang, H., Hermodson, M., and Stauffacher, C. (1998). Powering the ABC transporter: the 2.5A crystallographic structure and the ABC domain of rbsA. Pediatr. Pulmonol. Suppl. *17*, 91–92.

Ausubel, F.M., et al. (1993). Current Protocols in Molecular Biology (New York: Greens Publishing Associates, Inc., and John Wiley & Sons, Inc.).

Crawford, I., Maloney, P.C., Zeitlin, P.L., Guggino, W.B., Hyde, S.C., Turley, H., Gatter, K.C., Harris, A., and Higgins, C.F. (1991). Immunocytochemical localization of the cystic fibrosis gene product CFTR. Proc. Natl. Acad. Sci. USA *88*, 9262–9266.

Denning, G.M., Ostedgaard, L.S., Cheng, S.H., Smith, A.E., and Welsh, M.J. (1992). Localization of cystic fibrosis transmembrane conductance regulator in chloride secretory epithelia. J. Clin. Invest. *89*, 339–349.

Devidas, S., Yue, H., and Guggino, W.B. (1998). The second half of the cystic fibrosis transmembrane conductance regulator forms a functional chloride channel. J. Biol. Chem. *273*, 29373–29380.

Drumm, M.L., Pope, H.A., Cliff, W.H., Rommens, J.M., Marvin, S.A., Tsui, L., Collins, F.S., Frizzell, R.A., and Wilson, J.M. (1990). Correction of the cystic fibrosis defect *in vitro* by retrovirus-mediated gene transfer. Cell *62*, 1227–1233.

Eskandari, S., Wright, E.M., Kreman, M., Starace, D.M., and Zampighi, G.A. (1998). Structural analysis of cloned plasma membrane proteins by freeze-fracture electron microscopy. Proc. Natl. Acad. Sci. USA *95*, 11235–11240.

Frizzell, R.A., Rechkemmer, G., and Shoemaker, R.L. (1986). Altered regulation of airway epithelial cell chloride channels in cystic fibrosis. Science *233*, 558–560.

Gadsby, D.C., Nagel, G., and Hwang, T.C. (1995). The CFTR chloride channel of mammalian heart. Annu. Rev. Physiol. *57*, 387–416.

Hall, R.A., Ostedgaard, L.S., Premont, R.T., Blitzer, J.T., Rahman, N., Welsh, M.J., and Lefkowitz, R.J. (1998). A C-terminal motif found in the β_2-adrenergic receptor, P2Y1 receptor and cystic fibrosis transmembrane conductance regulator determines binding to the Na^+/H^+ exchanger regulatory factor family of PDZ proteins. Proc. Natl. Acad. Sci. USA *95*, 8496–8501.

Hillier, B.J., Christopherson, K.S., Prehoda, K.E., Bredt, D.S., and Lim, W.A. (1999). Unexpected modes of PDZ domain scaffolding revealed by structure of nNOS-syntrophin complex. Science *284*, 812–815.

Hung, L.W., Wang, I.X., Nikaido, K., Liu, P.Q., Ames, G.F., and Kim, S.H. (1998). Crystal structure of the ATP-binding subunit of an ABC transporter . Nature *396*, 703–707.

Kennedy, M.B. (1995). Origin of PDZ (DHR, GLGF) domains. Trends Biochem. Sci. *20*, 350.

Kim, E., Niethammer, M., Rothschild, A., Jan, Y.N., and Sheng, M. (1995). Clustering of Shaker-type K^+ channels by interaction with a family of membrane-associated guanylate kinases. Nature *378*, 85–88.

Kocher, O., Comella, N., Tognazzi, K., and Brown, L.F. (1998). Identification and partial characterization of PDZK1: a novel protein containing PDZ interaction domains. Lab. Invest. *78*, 117–125.

Kornau, H.C., Schenker, L., Kennedy, M., and Seeburg, P. (1995). Domain interaction between NMDA receptor subunits and the postsynaptic density protein PSD-95. Science *269*, 1737–1740.

Li, M., Unwin, N., Stauffer, K., Jan, Y.N., and Jan, L.Y. (1994). Images of purified shaker potassium channels. Curr. Biol. *4*, 110–115.

Marshall, J., Fang, S., Ostedgaard, L.S., O'Riordan, C.R., Ferrara, D., Amara, J.F., Hoppe, H., Scheule, R.K., Welsh, M.J., and Smith, A.E. (1994). Stoichiometry of recombinant cystic fibrosis transmembrane conductance regulator in epithelial cells and its functional reconstitution into cells in vitro. J. Biol. Chem. *269*, 2987–2995.

Rich, D.P., Anderson, M.P., Gregory, R.J., Cheng, S.H., Paul, S., Jefferson, D.M., McCann, J.D., Klinger, K.W., Smith, A.E., and Welsh, M.J. (1990). Expression of cystic fibrosis transmembrane conductance regulator corrects defective chloride channel regulation in cystic fibrosis airway epithelial cells. Nature *347*, 358–363.

Riordan, J.R., Rommens, J.M., Kerem, B.-S., Alon, N., Rozmahel, R., Grzelczak, Z., Zielenski, J., Lok, S., Plavsic, N., Chou, J.-L., et al. (1989). Identification of the cystic fibrosis gene: cloning and characterization of complementary DNA. Science *245*, 1066–1073.

Rosenberg, M.F., Callaghan, R., Ford, R.C., and Higgins, C.F. (1997). Structure of the multidrug resistance P-glycoprotein to 2.5 nm resolution determined by electron microscopy and image analysis. J. Biol. Chem. *272*, 10685–10694.

Shen, B.Q., Finkbeiner, W.E., Wine, J.J., Mrsny, R.J., and Widdicombe, J.H. (1994). Calu-3: a human airway epithelial cell line that shows cAMP-dependent Cl- secretion. Am. J. Physiol. *266*, L493–501.

Sheng, M. (1996). PDZs and receptor/channel clustering: rounding up the latest suspects. Neuron *17*, 575–578.

Short, D., Trotter, K., Reczek, D., Kreda, S., Bretscher, A., Boucher, R., Stutts, M., and Milgram, S. (1998). An apical PDZ protein anchors the cystic fibrosis transmembrane conductance regulator to the cytoskeleton. J. Biol. Chem. *273*, 19797–19801.

Songyang, Z., Fanning, A.S., Fu, C., Xu, J., Marfatia, S.M., Chishti, A.H., Crompton, A., Chan, A.C., Anderson, J.M., and Cantley, L.C. (1997). Recognition of unique carboxyl-terminal motifs by distinct PDZ domains. Science *275*, 73–77.

Stricker, N., Christopherson, K., Yi, B., Schatz, P., Raab, R., Dawes, G., Bassett, J., D., Bredt, D., and Li, M. (1997). PDZ domain of neuronal nitric oxide synthase recognizes novel C-terminal peptide sequences. Nat. Biotech. *15*, 336–342.

Trezise, A.E., and Buchwald, M. (1991). In vivo cell-specific expression of the cystic fibrosis transmembrane conductance regulator. Nature *353*, 434–437.

van Huizen, R., Miller, K., Chen, D.-M., Li, Y., Lai, Z.-C., Raab, R.W., Stark, W.S., Shortridge, R.D., and Li, M. (1998). Two distantly positioned PDZ domains mediate multivalent INAD-phospholipase C interactions essential for G protein-coupled signaling. EMBO J. *17*, 2285–2297.

Wang, S., Raab, R.W., Schatz, P.J., Guggino, W.B., and Li, M. (1998). Peptide binding consensus of the NHE-RF-PDZ1 domain matches the C-terminal sequence of cystic fibrosis transmembrane conductance regulator (CFTR). FEBS Lett. *427*, 103–108.

Wine, J.J. (1995). Cystic fibrosis: How do CFTR mutations cause cystic fibrosis? Curr. Biol. *5*, 1357–1359.

Zerhusen, B., Zhao, J., Xie, J., Davis, P.B., and Ma, J. (1999). A single conductance pore for chloride ions formed by two cystic fibrosis transmembrane conductance regulator molecules. J. Biol. Chem. *274*, 7627–7630.

Zielenski, J., and Tsui, L.C. (1995). Cystic fibrosis: genotypic and phenotypic variations. Annu. Rev. Genet. *29*, 777–807.